Supplementary information

1. Model and equation for T_1 and T_2 relaxometry

Water relaxation in hydrogels was obtained using a saturation recovery pulse sequence (SatRec) and Carr–Purcell–Meiboom–Gill sequence (CPMG), which are widely applied for measuring the T_1 and T_2 signals, respectively, of target molecules[49, 50]. The signal was integrated and then fitted with a three-parameter fitting model. T_i, i=1 or 2, is the relaxation value of the SatRec and CPMG fitting equation (equation S1), where t is the time of the measurement; A and B are the fitting parameters. The rotational correlation time (τ_c) of bound water can be estimated using the Solomon–Bloembergen equations (equations S2 and S3) and were approximated between 10^{-8} to 10^{-10} s for bound water τ_c estimation; this would be faster for average water τ_c. Specifically, regarding *C* in equations S2 and S3, γ is the gyromagnetic ratio of the hydrogen nucleus, h = Planck's constant (6.626×10^{-34} J s), $\hbar$ = h/2π, and *r* is the distance between the protons in the water molecule[27]. Water behaviour mostly follows $\omega_L\tau_c << 1$, so that equations S2 and S3 can be simplified to equation S4. This model had been employed to describe the relationship between polymer concentration and τ_c in PEG hydrogels [31].

Theoretically, τ_c can further be determined via the Stokes–Einstein–Debye equation (equation S6) to calculate the microviscosity of water, as well as cargo such as antibiotics and proteins[51]. The translational diffusion coefficient (*D*) can further be calculated via the Stokes–Einstein equation (equation S7). Here, η is the microviscosity of the surrounding medium, *r* is the hydrodynamic radius of the target molecules (herein water), *K* is Boltzmann's constant, and *T* is the temperature. However, in terms of the SED relationship, it is originally assumed that the analytes are in a dilute solution with a weak interactive force to crudely demonstrate the existence of a relationship between the hydrodynamic radii and diffusivity. The error of estimation would be further magnified in the hydrogel system while directly introducing SED on τ_c , calculated from the relaxation time solely, and neglects other parameters/forces. A further comparison experiment, such as pulsed field gradient NMR (PFG-NMR) on mobile water diffusivity[52, 53] and neutron scattering on slow dynamics of different waters (*tightly bound* and *intermediate* water)[54] would be necessary to improve the model.

2. Model and equation for $T_1\rho$ and K_{ex}

The dispersion of $R_1\rho$ versus spin lock strength was fitted using the Lorentzian model (equation S5), where R_2 and R_{2ex} are the transverse relaxation rates of the free exchanging pool (herein GelMA, GelMA_HAMA, or dECM polymer). Parameters ρ_{ex}, K_{ex} and Δw_0 denote the exchanging pool fractional population, exchange rate (from exchanging to water pool), and the chemical shift term, respectively, and w_1 is the spin-locking field amplitude ($w_1 = 2\pi \times$ spin lock frequency)[29].

$$F = A \cdot exp(-t/T_i) + B \tag{S1}$$

$$\eta \cdot \frac{2}{3} \cdot C\left(\frac{\tau_c}{1+\omega_L^2\tau_c^2} + \frac{4\tau_c}{1+4\omega_L^2\tau_c^2}\right) = \frac{1}{T_1} - \frac{1}{T_{1f}} = \Delta\left(\frac{1}{T_1}\right);\ C = \frac{9\gamma^4\hbar^2}{20r^6} \tag{S2}$$

$$\eta \cdot C\left(\tau_c + \frac{5\tau_c}{3(1+\omega_L^2\tau_c^2)} + \frac{2\tau_c}{3(1+4\omega_L^2\tau_c^2)}\right) = \frac{1}{T_2} - \frac{1}{T_{2f}} = \Delta\left(\frac{1}{T_2}\right);\ C = \frac{9\gamma^4\hbar^2}{20r^6} \tag{S3}$$

$$\frac{1}{T_2} = \frac{3}{2}\left(\frac{\gamma^4\hbar^2}{r^6}\right)\tau_c \tag{S4}$$

$$R_{1\rho} = R_2 + p_{ex}\left[R_{2ex} + \frac{k_{ex}\Delta w_0^2}{k_{ex}^2 + \Delta w_0^2 + w_1^2}\right] \tag{S5}$$

$$\tau_c = \frac{4\pi\eta r^3}{3kT} \tag{S6}$$

$$D = \frac{\kappa T}{6\pi\eta r} \tag{S7}$$

3. Microviscosity and diffusion coefficient of water in dECMMA hydrogels

Microviscosity of water in CarMA increased from $7 \pm 0.4 \times 10^{-3}$ (1%) to $9 \pm 0.6 \times 10^{-3}$ Pa·s. (2%); LungMA increased from $9 \pm 0.3 \times 10^{-3}$ (1%) to $1.3 \pm 0.1 \times 10^{-2}$ Pa·s (2%); BoneMA increased from $7 \pm 0.5 \times 10^{-3}$ (1%) to $9 \pm 0.1 \times 10^{-3}$ Pa·s (2%) (Fig. S1A). Conversely, the diffusion coefficient of CarMA decreased from 206.77 ± 11.87 (1%) to 164.71 ± 10.49 $\mu m^2 s^{-1}$ (2%); LungMA decreased from 154.62 ± 5.02 (1%) to 108.17 ± 4.39 $\mu m^2 s^{-1}$ (2%); BoneMA decreased from 222.09 ± 16.13 (1%) to 166.92 ± 11.83 $\mu m^2 s^{-1}$ (2%) (Fig. S1B).

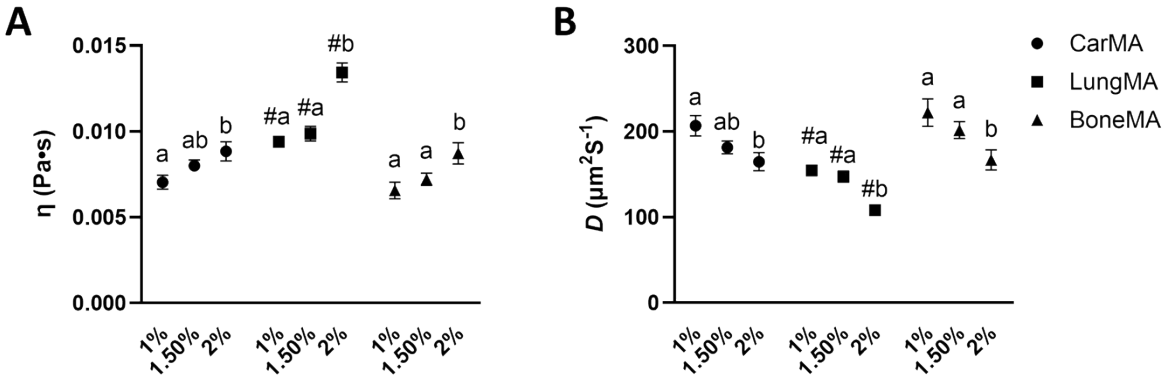

Figure S1. Microviscosity (A) and translational diffusion coefficient (B) values of water in 1, 1.5, and 2% CarMA, LungMA, and BoneMA hydrogels. a, b and # identify significant differences (p <0.05) among groups.

4. Appearance of dECMMA hydrogels

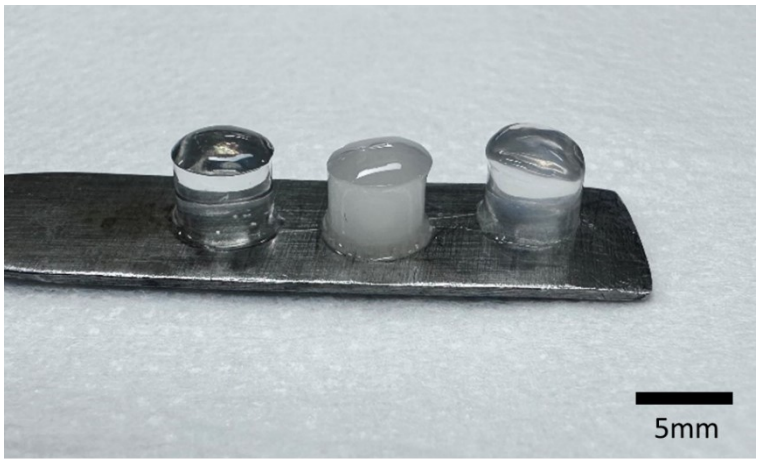

Figure S2. Appearance of 2% CarMA (left), LungMA (middle), and BoneMA (right). Transparent hydrogel of CarMA and BoneMA, and turbid LungMA. The transparency shows no significant difference before/after photo-crosslinking.

5. Mechanical properties of dECM hydrogels

5.1 Methods and instrument settings

The confined compression mechanical properties were conducted with an Instron 68TM-30 (Instron, USA) system equipped with a 5 N load cell and controlled with the Bluehill® software (Instron). Hydrogel samples were placed into a 3D-printed confined sample holder installed on the load cell. Hydrogels were hydrated with PBS at room temperature during the entire measurement. Compression was applied at a constant rate of 1 mm/min, initiating from a distance of 5 mm above the bottom of the load cell, and terminating either when a displacement of 0.1 mm was reached or the failure of the sample occurred. Force and displacement data were recorded and then converted into stress–strain data, as well as Young's modulus analysis with MATLAB code, generally by the following steps.

The initial height (L_0) of each hydrogel was measured by detecting the point at which a change in force was first recorded during the compression setup. The threshold for each sample was selected according to the material: for CarMA, 1%, 1.5% and 2%, 0.005, 0.0075 and 0.01 N, respectively; for BoneMA, 1%, 1.5% and 2%, 0.01, 0.025 and 0.025N, respectively, and for LungMA, 1%, 1.5% and 2%, 0.005, 0.01 and 0.025, respectively.

Strain (ε) was then calculated using the corresponding displacement (d_x) and the L_0, according to equation S8.

$$\varepsilon(\%) = \left(1 - \frac{d_x}{L_0}\right) \times 100 \quad \text{(S8)}$$

The stress (σ) was calculated using the applied force (F_x) and the contact area (A) according to equation S9.

$$\sigma = \frac{F_x}{A} \quad \text{(S9)}$$

The area used for the calculation was the bottom surface of the hydrogel, which was 19.63 mm². The program automatically picked the linear region of the stress–strain curve in the 10–20% region when compressing 0.5 mm into the sample. The compressive modulus (E) was determined as the slope of the linear region using equation S10.

$$E = \frac{\varepsilon_{20} - \varepsilon_{10}}{\sigma_{20} - \sigma_{10}} \quad \text{(S10)}$$

ε_{10} and ε_{20} represent the strain in the 10% and 20% deformation regions, respectively. σ_{10} and σ_{20} represent the corresponding stress values.

5.2 Results for mechanical properties of dECM hydrogels

The Young's modulus of CarMA increased from 3.59 ± 0.80 kPa (1%) to 12.92 ± 1.77 kPa (2%); LungMA increased from 56.04 ± 4.59 kPa (1%) to 86.89 ± 7.09 kPa (2%); BoneMA increased from 80.39 ± 9.07 kPa (1%) to 200.4 ± 77.01 kPa (2%) (Figure S3B).

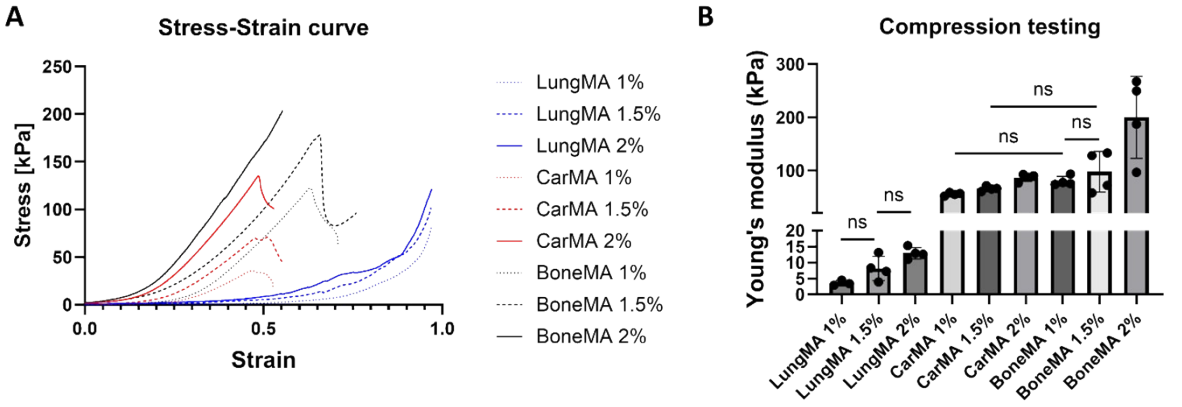

Figure S3. Stress–strain curve (A) and Young's modulus (B) of CarMA, LungMA, and BoneMA, 1, 1.5, and 2%; n=4